Journal of Hazardous Materials 383 (2020) 121133

Contents lists available at ScienceDirect

Journal of Hazardous Materials

journal homepage: www.elsevier.com/locate/jhazmat

Dramatic enhancement effects of l-cysteine on the degradation of sulfadiazine in Fe^{3+}/CaO_2 system

Jian Lu[a], Tenghao Wang[a], Yi Zhou[a], Changzheng Cui[a,b], Zhimin Ao[c], Yanbo Zhou[a,b,*]

[a] State Environmental Protection Key Laboratory of Environmental Risk Assessment and Control on Chemical Process, East China University of Science and Technology, No. 130 Meilong Road, Shanghai, 200237, China

[b] Shanghai Institute of Pollution Control and Ecological Security, No. 1515 Zhongshan Second North Road, Shanghai, 200092, China

[c] Guangdong Key Laboratory of Environmental Catalysis and Health Risk Control, Institute of Environmental Health and Pollution Control, School of Environmental Science and Engineering, Guangdong University of Technology, Guangzhou, 510006, China

GRAPHICAL ABSTRACT

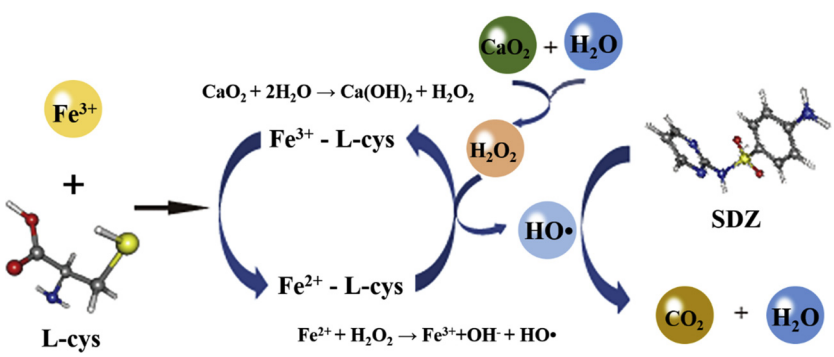

ARTICLE INFO

Editor: R. Teresa

Keywords:
Sulfadiazine
Calcium peroxide
l-cysteine
Fenton

ABSTRACT

Excessive sulfonamides accumulated in soil and groundwater seriously menace the ecological environment and human health. The performance of a Fenton-like system applying Fe^{3+} and calcium peroxide (CaO_2) in the presence of l-cysteine(l-cys) for sulfadiazine (SDZ) degradation was investigated. Compared with other chelating agents such as citric acid, butyric acid and Ethylenediaminetetraacetic acid, L-cys could effectively promote the SDZ removal in Fe^{3+}/CaO_2 system. With the addition of 0.5 mM l-cys, the SDZ degradation increased from 2.14% to 66.53% in 60 min. High concentration of HCO_3^- inhibited the degradation of SDZ while slightly negative effects on SDZ degradation were observed in the presence of Cl^- or humic acid (HA) in l-cys/Fe^{3+}/CaO_2 system. Electron paramagnetic resonance (EPR) analysis and radicals scavenge tests affirmed the generation of $^{\cdot}OH$ and O_2-$^{\cdot}$ in l-cys/Fe^{3+}/CaO_2 system. Possible degradation pathway of SDZ was speculated and the toxicity of SDZ intermediates was further evaluated. l-cys could enhance the reduction of Fe^{3+} to Fe^{2+} and reduced the Fe^{3+} precipitation due to the L-cys could form stable complexes with Fe^{3+}. L-cys/Fe^{3+}/CaO_2 system exhibited high mineralization ability. Overall, these results indicated that L-cys is a promising chelating agent for sulfadiazine wastewater treatment.

* Corresponding author at: State Environmental Protection Key Laboratory of Environmental Risk Assessment and Control on Chemical Process, East China University of Science and Technology, No. 130 Meilong Road, Shanghai, 200237, China.

E-mail addresses: zhouyanbo@ecust.edu.cn, hezi001007@163.com (Y. Zhou).

https://doi.org/10.1016/j.jhazmat.2019.121133
Received 8 August 2019; Received in revised form 28 August 2019; Accepted 31 August 2019
Available online 05 September 2019
0304-3894/ © 2019 Elsevier B.V. All rights reserved.

1. Introduction

Sulfonamides, a class of synthetic antibiotics, can inhibit growth and multiplication of bacteria through preventing folate synthesis, subsequent purine and DNA synthesis (Liu et al., 2019). Therefore, sulfonamides are widely employed for protecting human and livestock from diseases last decades (Peng et al., 2019). Nearly 6000 tons sulfonamides were used on livestock industries in 2013 according to the report from China, and among them, sulfadiazine (SDZ), one of typical sulfonamides, accounted for more than 15% (Zhang et al., 2015a). Unfortunately, up to 70%–90% of sulfonamides including SDZ were released into environment without effective treatment, and gradually accumulated in soil, groundwater or surface water on account of their recalcitrant and high-mobile property, posing potential threat on ecosystems (Bai et al., 2018). The undesirable existence of micropollutants could result in the acute or chronic toxicity on organisms, development of antibiotic resistant microorganisms and the emergence of antimicrobial – resistant bacteria pathogens and related genes (Liu et al., 2019; Yang et al., 2018a). These perniciousness and characteristics of non-biodegradability exerted potential threat on human, animals and ecosystem (Yang et al., 2018b). Realizing the threat of the micropollutants such as SDZ to ecosystem, some researchers have delved into removal methods.

Recently, advanced oxidation processes (AOPs) have been widely applied in degradation of SDZ, including Fenton and Fenton-like reactions (Zou et al., 2014), gamma irradiation (Rivas-Ortiz et al., 2017), ozonation (Garoma et al., 2010), ultrasonic oxidation (Lastre-Acosta et al., 2015), electrochemical activation (Nie et al., 2018) and photocatalytic methods (Zhou et al., 2017a; Cai et al., 2019). Additionally, Fenton reaction is considered as a promising technology for water remediation. Fenton reaction based AOPs exerts a large number of powerful oxidizing chemical substances, primarily hydroxyl radicals ($^{\cdot}OH$, standard oxidation potential of 2.8 V) by combination of iron ions and hydrogen peroxide (H_2O_2), as Eqs. (1) and (2). (Wang et al., 2017a)

$$Fe^{2+} + H_2O_2 \rightarrow Fe^{3+} + OH^- + HO^{\bullet} \quad k = 63\,M^{-1}s^{-1} \tag{1}$$

$$Fe^{3+} + H_2O_2 \rightarrow Fe^{2+} + HO_2^{\bullet} + H^+ \quad k = 0.002\,M^{-1} \tag{2}$$

However, the narrow pH operating range (pH 2–4) of Fenton reaction (Babuponnusami and Muthukumar, 2014; Zhou et al., 2017b) and instability characteristics of H_2O_2 (Zhang et al., 2018a) were limited to application in wastewater treatment. H_2O_2 cannot be exposed to the sunlight and the temperature cannot exceed 40℃ during transportation (Watts et al., 2007). Hence, some solid potent oxidants, such as MgO_2, ZnO_2 and CaO_2, were used to replace for H_2O_2 (Zhou et al., 2017b; Wu et al., 2019) because solid oxidants are more stable and convenient for transportation and storage. Compared with MgO_2 and ZnO_2, CaO_2 has drawn widespread concern in Fenton-like chemical oxidation due to its low price, non-toxic, environmentally-friendly properties and a long history of actual application in site remediation (Li et al., 2014). Contrastingly, ZnO_2 may cause second pollution due to the leakage of Zn^{2+}, a kind of heavy metal. Furthermore, MgO_2 can only be dissolved in dilute acid and insoluble in water, which greatly limits its application (Wu et al., 2019). Therefore, CaO_2 was chosen as the solid oxidant to replace liquid H_2O_2 in this text. Base on Eq. (3), CaO_2 can slowly decompose to release H_2O_2 in contact with water over a wide pH range of 3–11 (Wang et al., 2019a; Northup and Cassidy, 2008). And the yield of H_2O_2 increased as pH decreased to < 7 (Arienzo, 2000). Moreover, recent studies indicated that CaO_2 could be a more effective source of H_2O_2 than liquid H_2O_2 (Wang et al., 2017b). Liquid H_2O_2 is typically excessive added in Fenton system, but the utilization efficiency is not high which results in the waste of H_2O_2. However, the release rate of H_2O_2 from CaO_2 is slow, reducing disproportionation of H_2O_2 to O_2. Furthermore, Fe^{3+} was appropriate to catalyze CaO_2 due to the slower reaction rate of Fe^{3+} with H_2O_2 matches the rate of CaO_2 decomposition (Luo et al., 2016a; Zhou et al., 2017c). For example, Northup and Cassidy (2008) applied CaO_2 in modified Fenton chemistry and found that CaO_2 provided the 98% removal of tetrachloroethene (PCE), far more than the 31% degradation of PCE by liquid H_2O_2. In view of these, the application of CaO_2 in water body treatment and soil remediation was extensively investigated by researchers (Wang et al., 2019b). Zhang (Zhang et al., 2015b) reported that the degradation of trichloroethylene (TCE) could be effectively stimulated by ferrous ion/CaO_2 system and reach as high as 93.5%. Nevertheless, the oxidation efficiency was restricted by some intractable drawbacks, for instance, the slow reduction of Fe^{3+} to Fe^{2+} and fast precipitation of Fe^{3+} at pH > 4 (Dong et al., 2016).

$$CaO_2 + 2H_2O \rightarrow Ca(OH)_2 + H_2O_2 \tag{3}$$

To alleviate these negative effects, chelating agents, which can chelate metal ions by formation of complexes, have been applied in modified Fenton processes (Zhang et al., 2016a; Zhang et al., 2016b). Amina et al. (2018) investigated the performance of CaO_2/Fe^{2+}-EDTA system for Sulfamethoxazole removal at neutral pH. Additionally, Zhou (Zhou et al., 2017c) reported that Fe^{3+}/CaO_2 system accompanied by citric acid (CA) and tartaric acid (TA) could enhance the oxidation efficiency of bisphenol-A (BPA) and BPA degradation improved from 21.3% to 98.3% and 95.0% with 1.0 mM CA and TA, respectively.

Although chelating agents EDTA and CA could form stable complex with Fe^{3+} and reduce the amount of precipitation, these ligands lack the reducing ability to reduce Fe^{3+} to Fe^{2+}. Thus, reductants, such as ascorbic acid and hydroxylamine (HA) (Fukuchi et al., 2014), are introduced into the Fenton-like system to overcome the limitations of chelating agents. Lai et al. introduced HA into peroxymonosulfate/Fe_3O_4 system (Li et al., 2019) and oxidants/$CuFe_2O_4$ system (Yan et al., 2018), and the degradation efficiencies were greatly enhanced due to the accelerated Fe^{2+}/Fe^{3+} cycle by HA. However, it was reported that HA is toxic and may cause secondary pollution to the water body (Luo et al., 2016a). Compared with aforementioned chelating agents and reductants, l-cysteine(l-cys) presents excellent reducibility with a redox potential of about −350 mV and three active functional groups (−COOH, $-NH_2$ and −SH), reveals potent interactions with ferric and ferrous ion, thereby reduces the Fe^{3+} precipitation (Zhang et al., 2018b). On the other hand, l-cys, known as an important sulfur-containing amino acid, has no negative impact on environment (Luo et al., 2016a; Li et al., 2016). In addition, the complex of Fe^{3+}/ l-cys may provide a convenient channel for the transformation from Fe^{3+} to Fe^{2+} through internal redox caused by protonization (Luo et al., 2016a). On account of its above characteristics, l-cys could be employed in Fenton-like process to reduce the precipitation of Fe^{3+} and enhance the transmission between Fe^{3+} and Fe^{2+}. However, to our best knowledge, the assessment of L-cys acted as a chelating and reducing agent in Fe^{3+}/CaO_2 system for SDZ degradation has never been reported.

Therefore, the objective of this study was to estimate the oxidation property of Fe^{3+}- l-cys/CaO_2 system for SDZ degradation efficiency, which was extremely prospective. Four common chelating agents (l-cysteine(l-cys), citric acid (CA), butyric acid (BA) and Ethylenediaminetetraacetic acid (EDTA)) were firstly selected to compare the degradation performance of SDZ. Then, the conversion of ferrous and ferric ions in the presence of l-cys was investigated. In addition, electron paramagnetic resonance (EPR) analysis and radicals scavenge tests were used for determination of free radicals. The intermediates of SDZ degradation were determined and their toxicity was quantified by ECOSAR and T.E.S.T. Finally, in order to evaluate the potential application in wastewater treatment, the influences of solution matrix, such as Na^+, Mg^{2+}, Cl^-, HCO_3^- and NO_3^-, as well as natural organic matter (NOM) as humic acid were surveyed.

2. Materials and method

2.1. Materials

All chemicals were of analytical-reagent grade and used directly without further purification. Ferric sulfate ($Fe_2(SO_4)_3$, 99.5%) were purchased from Aaladdin Reagent Co. Ltd. Calcium peroxide (CaO_2, CP, 99.0%) was purchased from Macklin Biochemical Co., Ltd. Sulfadiazine ($C_{10}H_{10}N_4O_2S$, SDZ, 99.0%), l-cysteine ($C_3H_7NO_2S$, l-cys, 99.0%), citric acid (CA, 99.5%), isopropyl alcohol (IPA, 99.5%), chloroform (CF, 99.0%), tert-Butanol (TBA, 99.0%), sodium bicarbonate ($NaHCO_3$, 99.5%), Ethylenediaminetetraacetic acid (EDTA, 99.0%) and humic acid (HA) were purchased from Shanghai Titan Scientific Co., Ltd. Magnesium sulfate heptahydrate ($MgSO_4{\cdot}7H_2O$), butyric acid (BA, 99.0%), Sodium chloride (NaCl, 99.5%), 5,5-Dimethyl-1-pyrroline N-oxide (DMPO) and sodium sulfate (Na_2SO_4, 99.0%) were purchased from Shanghai Lingfeng Chemical Reagent Co., Ltd. Sodium nitrate ($NaNO_3$, 99.0%) were purchased from Sinopharm Chemical Reagent Co., Ltd.

2.2. Experiments procedures

A certain amount of Ferric sulfate and l-cys were firstly dissolved into SDZ solution (50 mg/L) and stirred in the reactors about 20 min for thorough dissolution. Followed by adding calcium peroxide to start the reaction and time. At the certain time intervals (at 0, 10, 20, 30, 45 and 60 min), 1.5 mL sample was taken out and filtered through a syringe filter (0.22 μm) as well as pH value was detected. Then, 0.20 mL methanol (HPLC) was added into the filtrate to terminate the Fenton reaction. The samples were collected and conserved for next detection. All the experiments were operated at room temperature (20.0 ± 2.0 °C) and the initial pH of SDZ solution was 6 ± 0.2 without adjustment. In order to reduce the usage of Fe^{3+}, 1.5 mM ferric sulfate and 2.0 mM calcium peroxide were decided, based on the best molar condition of Fe^{3+}/CaO_2 (3.0 mM/2.0 mM) in our previous work (Zhou et al., 2017c).

The purpose of free radicals scavenge test was to identify and evaluate the contribution of the oxygen species on SDZ degradation. IPA and CF were commonly employed as radical scavengers due to their high reactive activities with $^{\cdot}OH$ and $O_2^{-\cdot}$ potentially present in this system (Bing et al., 2013).

For EPR analysis, 1.0 mL DMPO was directly dissolved into 9.0 mL samples at the desirable time in the presence/absence of methanol. The mixed samples were transferred to a capillary tube immediately for next detection.

All working solutions were prepared with deionized water.

2.3. Analytical methods

The quantification of SDZ was determined by high performance liquid chromatography (HPLC, Hitachi, L-2000), outfitted with a multiple wavelength UV diode array detector set at 278 nm and a C18 column (Shimadzu, Japan). 10 μL each of samples was injected with the mobile phase of methanol and ultra-pure water in 60/40 vol ratio at a flow rate of 1.0 mL/min. Free ferrous ions and total iron was quantified by 1, 10 – Phenanthroline spectrophotometry method (Jiang et al., 2017). The absorbance of Fe^{2+} and total Fe were obtained by UV–vis spectrophotometer (type 2802, Unico Corp, China). The pH value was determined by using a pH meter (STARTER 2100). Total organic carbon (TOC) was analyzed by TOC analyzer (TOC-VCPH, Shimadzu, Japan).

EPR spectra was recorded on an EMX-8 spectrometer (Bruker Daltonics Inc., America) for determination of radical species. The operating conditions were as following: The sweep width and sweep time were fixed at 150 G and 41.94 s, respectively. The microwave power was set at 6.428 mW. Modulation frequency and modulation amplitude were set at 100 kHz and 1 G, respectively.

The intermediates of SDZ were analyzed by using LC–MS (Agilent 6120B). The mobile phase of LC was mixed with (A) 2.0 mM ammonium formate in water and (B) acetonitrile at a flow rate of 0.4 mL/min. The column temperature was set at 40 °C. The sample detection of MS equipped with electrospray ionization source (ESI) was operated in the positive and negative ion mode.

2.4. Evaluation of ecotoxicity

The Ecological Structure Activity Relationship (ECOSAR) program is validated and developed by EU and USEPA (Yang et al., 2018b), besides the Toxicity Estimation Software Tool (T.E.S.T.) is an Environmental Protection Agency online available computerized predictive system based on Quantitative Structure Activity Relationships (QSAR) (Lassalle et al., 2014). In this work, the acute and chronic toxicities of SDZ and its oxidation intermediates to three aquatic organisms, including fish, daphnid and green algae were estimated based on Neutral Organic SAR in ECOSAR. In addition, bioaccumulation factor, developmental toxicity and mutagenicity of these products were calculated by T.E.S.T. (Cai et al., 2019)

2.5. Statistical analysis

All experimental results are presented as mean values from three repetitions. One-way analysis of variance (ANOVA) was applied to compare the difference of the experimental data using Microsoft Office Excel 2016, and statistical difference was assumed when significant $p < 0.05$.

3. Result and discussion

3.1. Evaluation of l-cys chelating Fe^{3+}/CaO_2 system on SDZ degradation

In order to examine the potential effects of l-cys on SDZ removal in Fe^{3+}/CaO_2 system, series of comparative experiments were conducted to estimate the performance of SDZ degradation in the presence/absence of different chelating agents under same conditions.

The degradation efficiency of SDZ and the variation of pH values with/without chelating agents were presented in Fig. 1a and b. As seen from Fig. 1a, only 2.14% SDZ was removed in Fe^{3+}/CaO_2 system when without adding any chelating agents. In addition, with the continuation of the reaction time, pH value gradually increased from 3.32 to 7.23, as shown in Fig. 1b. CaO_2 generating calcium hydroxide in contact with water resulted in the pH values increased and the neutral or alkaline condition was adverse to radicals formation and organics oxidation, which might be the main reason for the poor performance of SDZ decontamination (Dias et al., 2016). The introduction of EDTA or BA had negligible effect on the degradation of SDZ in this system, less than 5% SDZ was degraded, which indicated that EDTA and BA might hold inferior chelation in this system. SDZ removal was efficiently promoted from 2.14% to 63.78% after 60 min reaction by adding the chelating agent of CA, and the operating pH values kept between 3 to 4, which was regarded as an optimal pH condition for Fenton reaction (Yu et al., 2016).

However, the satisfying oxidation performance for SDZ degradation was obtained by adding l-cys in Fe^{3+}/CaO_2 system. In the first 60 min, about 66.53% SDZ was removed in the presence of 0.5 mM l-cys and pH values increased regularly from 3.26 to 6.23. After 60 min reaction, the degradation of SDZ kept almost constant when adding CA or l-cys and the removal efficiency was very close (approximately 67.5%). In the first 60 min, the degradation efficiency of SDZ obviously increased with time in $CA/Fe^{3+}/CaO_2$ system and after 60 min reaction, the degradation efficiency kept constant which may be ascribe to the limited production of H_2O_2. Meanwhile, the degradation rate of SDZ was very fast in the first 10 min in $l\text{-}cys/Fe^{3+}/CaO_2$ system and the degradation efficiency of SDZ was weakly improved in next reaction. It was

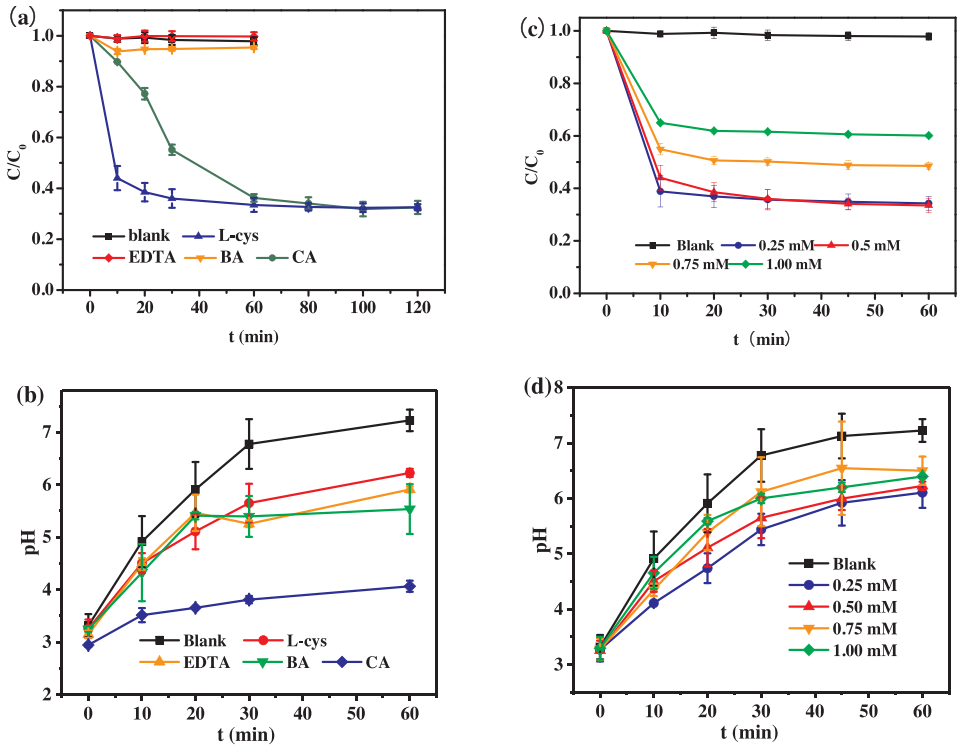

Fig. 1. Effects of different chelating agents on (a) SDZ degradation, (b) pH values and effects of l-cys concentrations on (c) SDZ degradation, (d) pH values in Fe^{3+}/CaO_2 system. $[SDZ]_0 = 50$ mg/L, $[Fe^{3+}]_0 = 1.5$ mM, $[CaO_2]_0 = 2.0$ mM, initial pH = 6 ± 0.2, T = 20 °C.

concluded that the chelating agent l-cys has strong reduction which rapidly reduces Fe^{3+} to Fe^{2+} (Luo et al., 2016a). The strong reduction of l-cys makes the reaction rate of l-cys/Fe^{3+}/CaO_2 much higher than that of CA/Fe^{3+}/CaO_2 system. The above results showed that the addition of l-cys can significantly shorten the reaction time compared with adding CA. Compared with other three chelating agents, the superior catalytic oxidation capacity of SDZ decontamination and wider working pH range were the advantages of l-cys in Fe^{3+}/CaO_2 system. The Fenton-cys system revealed a more rapid reaction rate constant than traditional Fenton system and the oxidant consumption index of Fenton-cys system was lower than that of traditional Fenton system (Luo et al., 2016b), meaning a preferable utilization efficiency of H_2O_2. These above evidences supported the effective oxidation of SDZ by adding l-cys in Fe^{3+}/CaO_2 system.

To further determine the optimal level of l-cys for SDZ removal, the tests were carried out with different l-cys concentrations in Fe^{3+}/CaO_2 system. The results of SDZ removal efficiency and the pH changes with 0.00, 0.25, 0.50, 0.75 and 1.00 mM L-CYS WERE EXHIBITED INFig. 1c and d, respectively. From Fig. 1c, the increasing of l-cys usage could dramatically facilitate the degradation of SDZ at the beginning, but an inhibition of SDZ degradation was observed with much more l-cys added. More than 65% SDZ were eliminated in the presence of 0.50 mM l-cys, while 0.75 mM and 1.00 mM L-cys only remove 51.47% and 39.90%, respectively. It could be deduced that the restriction on SDZ degradation might be due to the competition of chelating agents as l-cys with SDZ for Fenton-like oxidation (Lin et al., 2017). For the convenience of l-cys addition, 0.50 mM l-cys was selected in following experiments. Furthermore, regardless of the test dosage of l-cys, the operating pH increased with the reaction time and the final pH value kept at around 6, as shown in Fig. 1d, which manifested that l-cys could expend the effective pH range for Fenton system.

Hence, the experimental results presented above revealed that the addition of l-cys could significantly promote the degradation efficiency of SDZ in Fe^{3+}/CaO_2 system due to its excellent reduction ability and exert a satisfactory pH adaptability for Fenton-like reaction. Compared with other chelating agents, l-cys is type of promising chelating agent for wastewater treatment, although its application is not yet mature. The application of l-cys in practical process still needs more in-depth and detailed research to further optimize the dosage and other parameters in order to achieve more economic and efficient.

For further exploring the mechanisms of l-cys in Fenton reaction, 0.50 mM l-cys was employed in 1.5 mM Fe^{3+} and 2.0 mM CaO_2 system for the following experiments.

3.2. Conversion of Fe^{3+} and Fe^{2+} in L-cys/Fe^{3+}/CaO_2 system

To survey the influence of l-cys on the valance state of iron ions, the transformations of ferrous and ferric iron in the absence/presence of 0.5 mM l-cys under the conditions of 1.5 mM Fe^{3+} and 2.0 mM CaO_2 were investigated and demonstrated in Fig. 2a and b, respectively. From Fig. 2a, the concentration of ferric iron maintained constant before the Fenton reaction in the solution. With the addition of CaO_2, the Fenton reaction began, and a small amount of ferrous iron gradually generated due to the conversion of ferric iron. However, no more than 0.1 mM ferrous iron was found during the Fenton-like reaction. For example, only 0.04 mM ferrous iron was produced at 10 min of reaction. The tiny concentration of ferrous iron, which could be the main reason for poor SDZ degradation performance in Fe^{3+}/CaO_2 system, might be associated with the rapid consumption in reaction with H_2O_2 and slow reduction of Fe^{3+} to Fe^{2+} (Dong et al., 2016). In addition, the total soluble iron ions were decreased from initial 1.50 mM to 1.04 mM at the end of the reaction. Near 30% iron ions might aggregate and form insoluble complexes owing to the fast precipitation of Fe^{3+} (Subramanian and Madras, 2017), leading to a large loss of iron.

As seen in Fig. 2b, a large amount of ferrous iron was rapidly generated along with the addition of l-cys. The concentration of ferrous iron increased from 0.04 to 0.71 mM after adding 0.5 mM l-cys. This significant conversion of Fe^{3+} to Fe^{2+} was attributed to the powerful reducibility of l-cys. After timing, the concentration of ferrous iron dropped sharply corresponding to the rise of ferric iron. For instance,

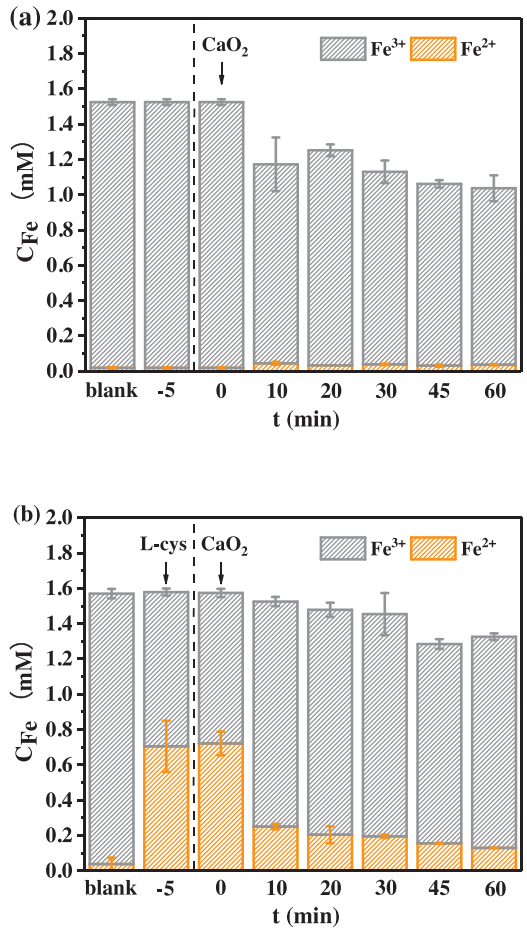

Fig. 2. Variation of Fe^{2+} and Fe^{3+} during the whole experiments (a) in the absence of l-cys, (b) in the presence of l-cys. $[SDZ]_0$ = 50 mg/L, $[Fe^{3+}]_0$ = 1.5 mM, $[CaO_2]_0$ = 2.0 mM, $[l\text{-cys}]_0$ = 0.5 mM, T = 20 °C.

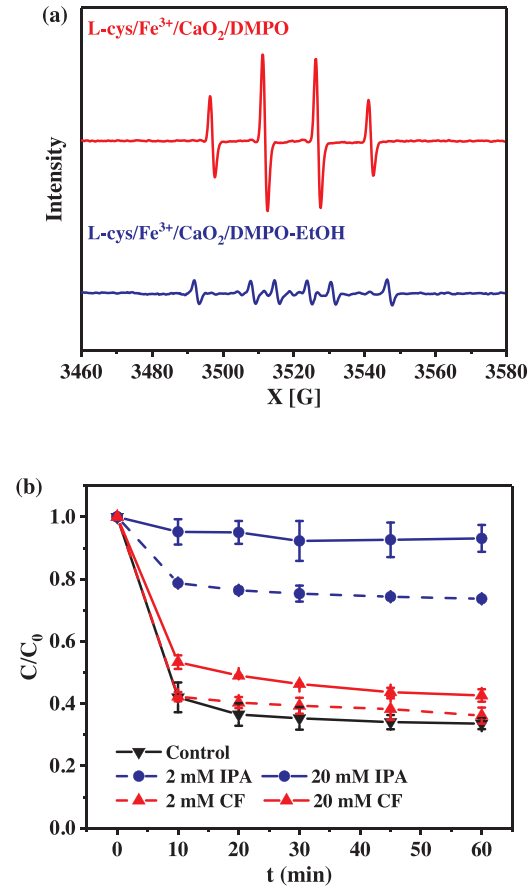

Fig. 3. (a) EPR spectra of l-cys/Fe^{3+}/CaO_2 system and (b) the effects of scavengers under different concentrations on SDZ removal in L-cys/Fe^{3+}/CaO_2 system. $[SDZ]_0$ = 50 mg/L, $[Fe^{3+}]_0$ = 1.5 mM, $[CaO_2]_0$ = 2.0 mM, $[l\text{-cys}]_0$ = 0.5 mM, T = 20 °C.

0.72 mM ferrous iron reduced to 0.25 mM in 10 min, which indicated that ferrous iron was converted into ferric iron through Fenton-like reaction (Rahim Pouran et al., 2014). As the reaction progressed, the amount of ferrous iron decreased from initial 0.72 to 0.25, 0.20, 0.20, 0.16 and 0.13 mM. The presence of ferrous iron might be the main reason for l-cys effectively enhancing the degradation of SDZ. Furthermore, at the end of the reaction, 0.25 mM iron ions were lost thanks to formation of precipitation in the solution. Hence, fewer iron ions were wasted in the presence of l-cys, compared with that in blank Fe^{3+}/CaO_2 system, which implied that the addition of l-cys could alleviate the generation of precipitation in Fe^{3+}/CaO_2 system.

Interestingly, as shown in Fig. 2, the total soluble iron was decreased from initial 1.50 mM to 1.04 mM which means that 0.46 mM iron ions were formed insoluble complexes or aggregated in Fe^{3+}/CaO_2 system. Meanwhile, only 0.25 mM ions were aggregated in l-cys/Fe^{3+}/CaO_2 system which was much lower than that of Fe^{3+}/CaO_2 system. Chelating agent l-cys can obviously reduce the generation of Fe^{3+} precipitation. However, as shown in Fig. 1c, the removal efficiency of SDZ in Fe^{3+}/CaO_2 system was only 2.14%, which was much lower than that of l-cys/Fe^{3+}/CaO_2 system (66.53%). Therefore, theoretically the percentage of SDZ removed by precipitation might be much lower than 2.14% due to the less precipitation formed in L-cys/Fe^{3+}/CaO_2 system than that in Fe^{3+}/CaO_2 system.

3.3. Identification of free radicals in l-cys/Fe^{3+}/CaO_2 system

The generation of $^{\cdot}OH$ and $O_2^{-\cdot}$ was reported in Fe^{3+}/CaO_2 system (Pan et al., 2018). To verify the presence of $^{\cdot}OH$ and $O_2^{-\cdot}$ in l-cys/Fe^{3+}/CaO_2 system, free radicals were monitored by EPR spectra and free radical scavenging tests. Fig. 3a presented the typical EPR spectrum. Four-lines of strong signals with a peak height ratio of 1: 2: 2: 1 were observed in l-cys/Fe^{3+}/CaO_2/DMPO system, which could be assigned to the characteristic signals of DMPO-$HO^{\cdot}$ adducts (with hyperfine splitting constants of $a_H = a_N = 14.89$ G) (Wang et al., 2015). These DMPO-$HO^{\cdot}$ signals might be ascribed to the formation of $HO^{\cdot}$ by activating CaO_2. Literature reported that IPA had reactivity with $^{\cdot}OH$ at a high rate of $k_{\dot{O}H} = 1.9 \times 10^9\ M^{-1}\ S^{-1}$ (Amina et al., 2018). The introduction of IPA brought a significant decline in SDZ degradation. As shown in Fig. 3b, as the amount of IPA increased from 2 to 20 mM, the degradation efficiency of SDZ dropped to 26.30% and 6.89%, respectively. The obvious decrease in SDZ removal might result from the scavenging effect on $^{\cdot}OH$, which suggested that a majority of SDZ degradation was ascribed to $^{\cdot}OH$ oxidation in this system.

Furthermore, inferior signals of DMPO-$O_2^{\cdot}$ adducts (with hyperfine splitting constants $a_N = 14.3$ G, $a_H = 11.2$ G, and $a_H = 1.3$ G) appeared in l-cys/Fe^{3+}/CaO_2/DMPO-EtOH system, which was similar to those in Qin's research (Qin et al., 2018), implying the presence of $O_2^{-\cdot}$. The results above confirmed that OH and $O_2^{-\cdot}$ coexisted in l-cys/Fe^{3+}/CaO_2 system (Wang et al., 2017b). CF was generally recommended as a scavenger for $O_2^{-\cdot}$ due to its minimal reactivity with $^{\cdot}OH$ ($k_{\dot{O}H} = 7 \times 10^6\ M^{-1}\ S^{-1}$) and high reaction rate constant with $O_2^{-\cdot}$ ($k_{\dot{O}H} = 3 \times 10^{10}\ M^{-1}\ S^{-1}$) (Zhang et al., 2015b). As adding 2 mM CF, negligible transformation in removal of SDZ was observed and 9.07% degradation efficiency of SDZ was inhibited in the presence of 20 mM CF from Fig. 3b, confirming that $O_2^{-\cdot}$ was generated and promoted the SDZ degradation in this system. Our results were in accordance with

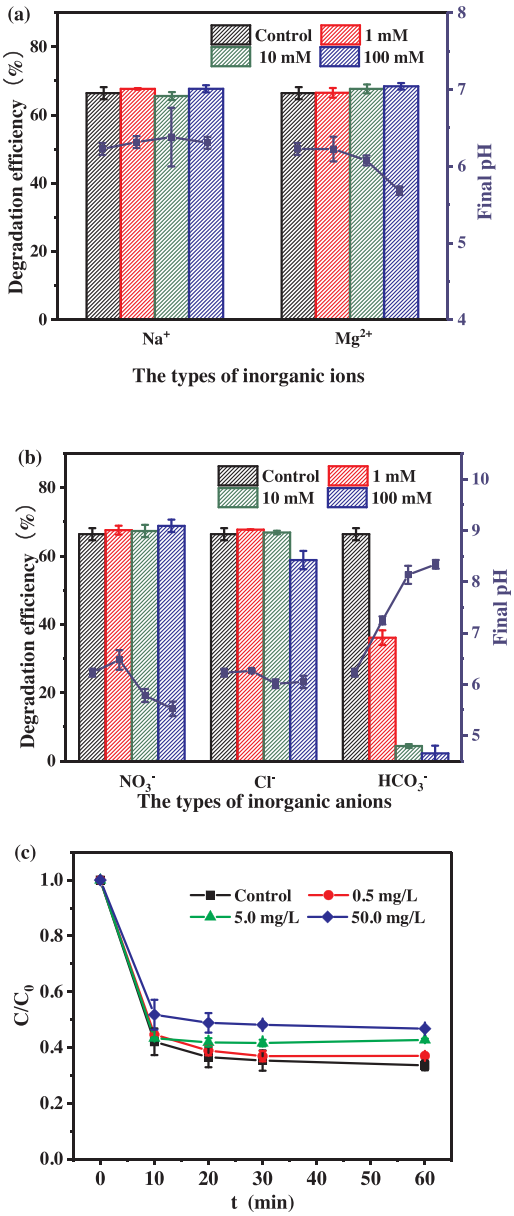

Fig. 4. Influences of (a) inorganic ions, (b) inorganic anions and (c) humic acid on SDZ removal and final pH values in L-cys/Fe^{3+}/CaO_2 system. $[SDZ]_0$ = 50 mg/L, $[Fe^{3+}]_0$ = 1.5 mM, $[CaO_2]_0$ = 2.0 mM, $[L\text{-cys}]_0$ = 0.5 mM, T = 20 °C.

previous report (Wang et al., 2017b).

In general, it was speculated that ˙OH made a major contribution to SDZ degradation and $O_2^{-\cdot}$ also enhanced SDZ removal although its role was limited. In addition, the results from free radical scavenging tests were consistent with the detection by EPR spectrum.

3.4. Effect of solution matrix on SDZ removal in l-cys/Fe^{3+}/CaO_2 system

3.4.1. Ions effect

A mass of inorganic ions e.g. Na^+, Mg^{2+}, Cl^-, HCO_3^- and NO_3^- were prevalent in livestock wastewater or antibiotic wastewater. The presence of these ions may affect the degradation of SDZ in l-cys/Fe^{3+}/CaO_2 system. Hence, the influences of ions and anions on SDZ removal were presented in Fig. 4a and b, respectively. All the experimental conditions were fixed in this section and the initial pH of SDZ solution was 6 ± 0.2 without adjustment. The pH values were measured from the start of the reactions.

Regardless of the amount of Na^+ or Mg^{2+}, no obvious variation on SDZ degradation efficiency appeared and final pH values were determined around 6.0, meaning unremarkable effect of Na^+ and Mg^{2+} on SDZ removal in l-cys/Fe^{3+}/CaO_2 system. In addition, less than 3% in the variation of SDZ degradation were signified in the presence of 1, 10 and 100 mM NO_3^-, similar results as the effect of Na^+ and Mg^{2+}.

Compared with these ions above, an apparent suppression on the degradation efficiency was detected with high Cl^- concentration. With the addition of 1 and 10 mM Cl^-, the degradations of SDZ were slightly affected and maintained around 67%, while SDZ removal decreased by about 8% in the presence of 100 mM Cl^-. It can be inferred that under high Cl^- concentration could inhibit the degradation efficiency by competitive consumption of ˙OH, accompanying the generation of two lower active radicals, as Eqs (Zhang et al., 2016b; Amina et al., 2018).

$$Cl^- + HO^\bullet \rightarrow ClOH^{\bullet-} \quad k=4.3\times10^9\,M^{-1}s^{-1} \tag{4}$$

$$ClOH^{\bullet-} + H^+ \rightarrow Cl^\bullet + H_2O \quad k=3.2\times10^{10}\,M^{-1}s^{-1} \tag{5}$$

$$Cl^- + Cl^\bullet \rightarrow Cl_2^{-\bullet} \quad k=7.8\times10^9\,M^{-1}s^{-1} \tag{6}$$

On the other hand, increasing the addition of HCO_3^- from 0 to 100 mM brought about the decline in SDZ removal from 66.43% to 36.13%, 4.40% and 2.25%, respectively. Then, the final pH values were increased above 7 and meant the alkalinity of solution. A possible explanation for this noteworthy inhibition on SDZ degradation was that the addition of HCO_3^- increased the operating pH values out of range of appropriate pH for Fenton reaction (Babuponnusami and Muthukumar, 2014) and HCO_3^- had scavenging effect with ˙OH to generate an inferior active radical as $CO_3^{-\cdot}$, as Eqs (Zhang et al., 2015b).

$$HCO_3^- + HO^\bullet \rightarrow CO_3^{-\bullet} + H_2O \quad k=8.5\times10^6\,M^{-1}s^{-1} \tag{7}$$

$$CO_3^{2-} + HO^\bullet \rightarrow CO_3^{-\bullet} + HO^- \quad k=3.9\times10^8\,M^{-1}s^{-1} \tag{8}$$

3.4.2. NOM effect

Natural organic matter (NOM) was ubiquitous in soil and water environment. Humic acid (HA) on behalf of organic matter was selected to assess the influence on SDZ degradation. From the Fig. 4c, as the increase addition of HA from 0 to 50 mg/L, the removal efficiency of SDZ was decreased from 66.43% to 63.03%, 57.28% and 53.27%. Similar phenomenon was observed in Fu's study (Fu et al., 2015). It was speculated that HA acting as a potential contaminant competed with SDZ leading to slow down the degradation efficiency. Therefore, the adverse influence of NOM should be concerned in the practical application.

3.5. Degradation pathways of SDZ by l-cys/Fe^{3+}/CaO_2 system

The oxidation intermediates were analyzed by LC–MS and the possible degradation pathways were speculated in Fig. 5. As mentioned in the previous report, the sites I to IV, representing H—N, N—C, N—S and N—C bonds in pyrimidine ring, might be the potential cleavage sites of SDZ, prone to be broke by free radicals (Rong et al., 2014). As a result, the H—N bond of SDZ was attacked by radicals and subsequently hydroxylated resulting in the formation of compound 1 with *m/z*286 (N-hydroxy-5-hydroxyl-SDZ). In addition, N—C bond of SDZ was broken for generating compound 2 with *m/z*237. Under the sequential attack of radicals, compound 1 and 2 were likely to convert to compound 4 with *m/z*200 (N-aminoiminomethyl-benzenesulfonamide). The generation of compound 3 with *m/z*214 (Sulfaguanidine) came from cleavage of the pyrimidine ring, where the two N—C bonds were unstable and easily broken, in accordance with Sun' research (Sun et al., 2018). Compound 4 underwent a subsequent attack by radicals, which destroyed the N—C and N—S bonds to produce compound 5 with *m/z*172 (Sulfanilamide) and compound 6 with *m/z*173 (Sulfanilic acid), respectively.

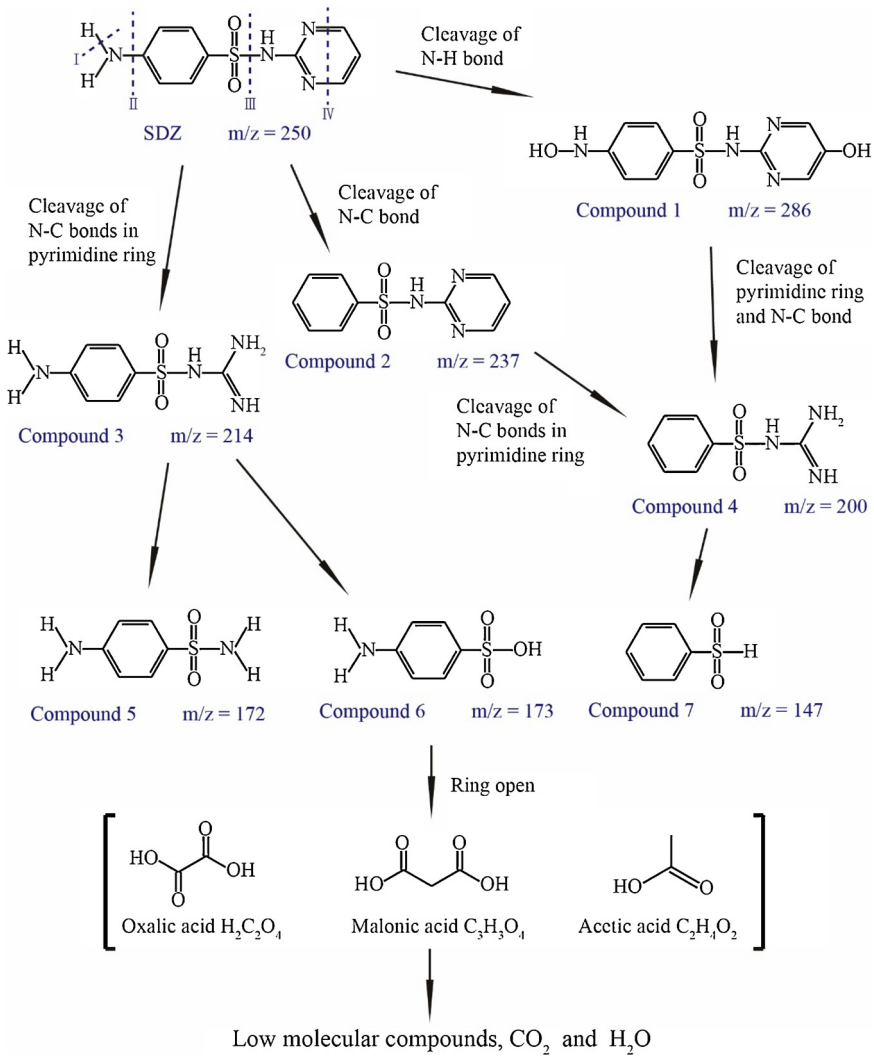

Fig. 5. Possible pathway for SDZ degradation in L-cys/Fe^{3+}/CaO_2 system.

Furthermore, the observation of compound 7 with *m/z*147 (Benzenesulfinic acid) was the product of compound 4, which suggested the cleavage of N—S bond. It was reported that these compounds were further degraded by free radicals leading to the formation of aliphatic carboxylic acid, finally transforming into carbon dioxide and water (Khankhasaeva et al., 2015).

3.6. Mineralization and toxicity assessment of SDZ and its intermediates in l-cys/Fe^{3+}/CaO_2 system

In order to evaluate the mineralization ability of l-cys/Fe^{3+}/CaO_2 system, TOC analysis under optimized conditions was conducted. Fig. 6 shows the TOC removal efficiency at different time in l-cys/Fe^{3+}/CaO_2 system. As the reaction time increases, the mineralization efficiency also increases. After 10 min reaction, the TOC removal efficiency reached 27.35% whereas TOC removal efficiency at 60 min was 33.45% which suggested that the mineralization reaction mainly occurs in the first 10 min. The result was consistent with the degradation efficiency of SDZ. The TOC removal efficiency illustrates that l-cys/Fe^{3+}/CaO_2 system possesses a good oxidation performance which might be ascribed to the radical pathway including $^{\cdot}OH$ and $O_2^{-\cdot}$.

However, the mineralization efficiency of l-cys/Fe^{3+}/CaO_2 system is not high. Some toxic intermediates may be formed during advanced oxidation processes. Thus, further increasing the degree of mineralization and reducing the potential toxicity of wastewater are of great

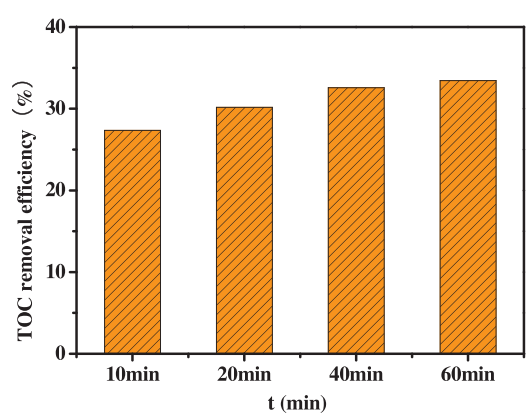

Fig. 6. TOC removal efficiency in L-cys/Fe^{3+}/CaO_2 system. $[SDZ]_0$ = 50 mg/L, $[Fe^{3+}]_0$ = 1.5 mM, $[CaO_2]_0$ = 2.0 mM, T = 20 °C.

significance for practical application. The reaction time and the ratio of oxidant to catalyst can be optimized to further improve the mineralization of Fenton/Fenton-like reactions. Subsequently, other technologies such as adsorption or photocatalytic degradation can be combined with Fenton/Fenton-like methods to further increase the pollutants removal efficiency and reduce the potential toxicity risk (Zhou et al., 2017a; Chen et al., 2019).

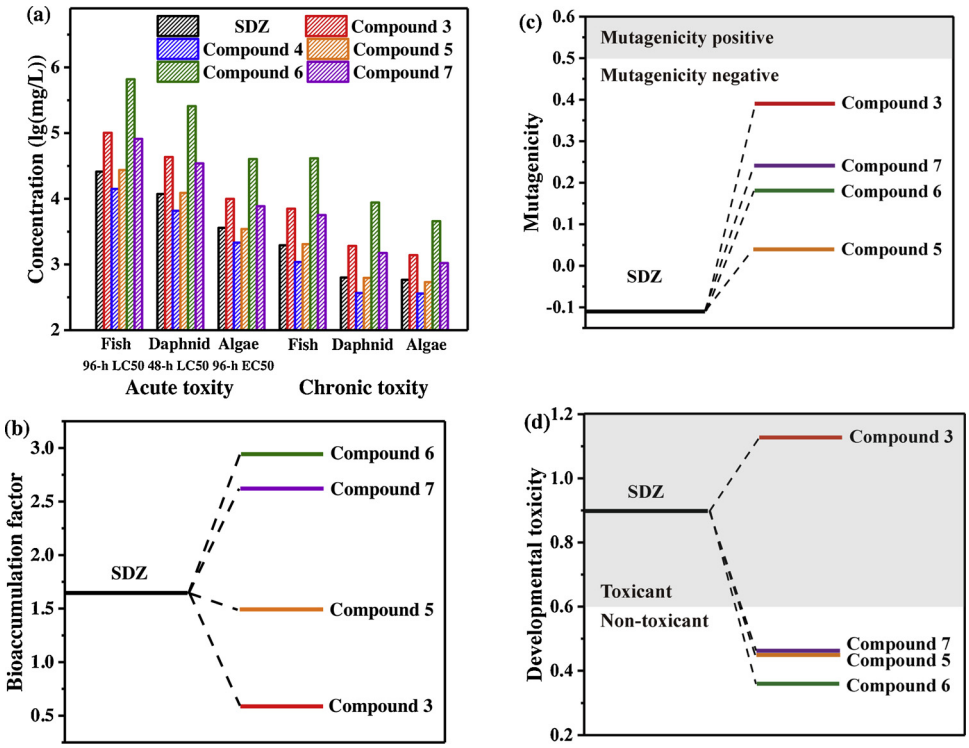

Fig. 7. (a) Predicted toxicity, (b) bioaccumulation factor, (c) mutagenicity and (d) developmental toxicity of SDZ and its degradation intermediates.

Meanwhile, the acute and chronic toxicity of SDZ and its oxidation intermediates to fish, daphnid and green algae were measured by ECOSAR based on the class of Neutral Organic SAR, while bioaccumulation factor, developmental toxicity and mutagenicity of these by-products were predicted by T.E.S.T. These results were exhibited in Fig. 7. Products such as compound 1 and 2 were not included in the database probably owing to poor stability. As shown in Fig. 7a, the LC_{50} of SDZ for fish and daphnid were calculated to be 25852 and 11829 mg/L, and EC_{50} values for green algae was 3609 mg/L. The chronic toxicity for fish, daphnid and green algae were calculated at 1959, 632 and 584 mg/L. Except for compound 4, acute and chronic toxicity of other compound were far more than those of SDZ, meaning that these intermediates were less toxic.

From Fig. 7b, compared with SDZ, the bioaccumulation factors of compound 6 and 7 were increased, while those of compound 3 and 5 were decreased, indicated that these intermediates were more easily enriched in living organisms. Mutagenicity of these intermediates were increased but these were categorized as "mutagenicity negative". Apart from compound 3, parameters of these intermediates were lower than that of original SDZ in developmental toxicity.

4. Conclusion

Conclusively, the effect of organic chelates on SDZ degradation in a Fenton-like reaction (Fe^{3+}/CaO_2) were systematically investigated. The SDZ degradation efficiency with different chelating agents follows the order: BA < EDTA < CA ≤ l-cys. The introduction of l-cys into Fe^{3+}/CaO_2 system could dramatically enhance the degradation efficiency of SDZ. Compared with adding CA, the addition of l-cys can significantly increase the reaction rate and shorten the reaction time. With the addition of 0.5 mM l-cys, nearly half of ferric iron was transformed to ferrous iron, which alleviated the drawback of the slow reduction of Fe^{3+} to Fe^{2+} consequently promoting SDZ degradation. The radicals of $^{\cdot}OH$ and $O_2^{-\cdot}$ were identified by EPR and free radical scavenging tests and $^{\cdot}OH$ made a major contribution to SDZ degradation while $O_2^{-\cdot}$ also played a limited role. Furthermore, a certain amount of Cl-, HCO_3- and HA could lead to passive influence on the SDZ degradation. From the evolution of these intermediates, the possible degradation pathways and their toxicity were suggested with special interest. In general, these results expressed that the l-cys/Fe^{3+}/CaO_2 system is a promising approach for remediation of SDZ contaminated wastewater.

Acknowledgements

This work was supported by the National Key Research and Development Program of China (Grant No. 2017YFB0602601), the National Natural Science Foundation of China (Grant No. 51778230), Shanghai Rising-Star Program (Grant No. 17QA1401000), and the Fundamental Research Funds for the Central Universities for their financial support(Grant No. 222201718003).

References

Amina, Si, X., Wu, K., Si, Y., Yousaf, B., 2018. Synergistic effects and mechanisms of hydroxyl radical-mediated oxidative degradation of sulfamethoxazole by Fe(II)-EDTA catalyzed calcium peroxide: implications for remediation of antibiotic-contaminated water. Chem. Eng. J. 353, 80–91.
Arienzo, M., 2000. Degradation of 2,4,6-trinitrotoluene in water and soil slurry utilizing a calcium peroxide compound. Chemosphere 40, 331–337.
Babuponnusami, A., Muthukumar, K., 2014. A review on Fenton and improvements to the Fenton process for wastewater treatment. J. Environ. Chem. Eng. 2, 557–572.
Bai, Y., Ruan, X., Wang, F., Antoine, G., van der Hoek, J.P., 2018. Sulfonamides removal under different redox conditions and microbial response to sulfonamides stress during riverbank filtration: a laboratory column study. Chemosphere 220, 668–677.
Bing, J., Wang, X., Lan, B., Liao, G., Zhang, Q., Li, L., 2013. Characterization and reactivity of cerium loaded MCM-41 for p-chlorobenzoic acid mineralization with ozone. Sep. Purif. Technol. 118, 479–486.
Cai, Z., Hao, X., Sun, X., Du, P., Liu, W., Fu, J., 2019. Highly active WO3@anatase-SiO2 aerogel for solar-light-driven phenanthrene degradation: mechanism insight and toxicity assessment. Water Res. 162, 369–382.
Chen, Q., Chen, L., Qi, J., Tong, Y., Lv, Y., Xu, C., Ni, J., Liu, W., 2019. Photocatalytic degradation of amoxicillin by carbon quantum dots modified K2Ti6O13 nanotubes: effect of light wavelength. Chin. Chem. Lett. 30, 1214–1218.
Dias, F.F., Oliveira, A.A.S., Arcanjo, A.P., Moura, F.C.C., Pacheco, J.G.A., 2016. Residue-based iron catalyst for the degradation of textile dye via heterogeneous photo-Fenton. Appl. Catal. B: Environ. 186, 136–142.
Dong, H., Sans, C., Li, W., Qiang, Z., 2016. Promoted discoloration of methyl orange in H_2O_2 /Fe(III) Fenton system: effects of gallic acid on iron cycling. Sep. Purif. Technol.

171, 144–150.
Fu, X., Gu, X., Lu, S., Miao, Z., Xu, M., Zhang, X., Qiu, Z., Sui, Q., 2015. Benzene depletion by Fe^{2+}-catalyzed sodium percarbonate in aqueous solution. Chem. Eng. J. 267, 25–33.
Fukuchi, S., Nishimoto, R., Fukushima, M., Zhu, Q., 2014. Effects of reducing agents on the degradation of 2,4,6-tribromophenol in a heterogeneous Fenton-like system with an iron-loaded natural zeolite. Appl. Catal. B 147, 411–419.
Garoma, T., Umamaheshwar, S.K., Mumper, A., 2010. Removal of sulfadiazine, sulfamethizole, sulfamethoxazole, and sulfathiazole from aqueous solution by ozonation. Chemosphere 79, 814–820.
Jiang, C., Yang, S., Gan, N., Pan, H., Liu, H., 2017. A method for determination of $[Fe^{3+}]/[Fe^{2+}]$ ratio in superparamagnetic iron oxide. J. Magn. Magn. Mater. 439, 126–134.
Khankhasaeva, S., Dambueva, D.V., Dashinamzhilova, E., Gil, A., Vicente, M.A., Timofeeva, M.N., 2015. Fenton degradation of sulfanilamide in the presence of Al, Fe-pillared clay: catalytic behavior and identification of the intermediates. J. Hazard. Mater. 293, 21–29.
Lassalle, Y., Jellouli, H., Ballerini, L., Souissi, Y., Nicol, E., Bourcier, S., Bouchonnet, S., 2014. Ultraviolet-vis degradation of iprodione and estimation of the acute toxicity of its photodegradation products. J. Chromatogr. A 1371, 146–153.
Lastre-Acosta, A.M., Cruz-Gonzalez, G., Nuevas-Paz, L., Jauregui-Haza, U.J., Teixeira, A.C., 2015. Ultrasonic degradation of sulfadiazine in aqueous solutions. Environ. Sci. Pollut. Res. Int. 22, 918–925.
Li, Y., Zhou, Y., Zhou, Zh., Wang, N., Zhou, Q., Wang, F., 2014. Effects of sustained-release composite on the oxygen levels and sediment phosphorus fractions of an urban river in Shanghai. Environ. Technol. 35 (17), 2176–2182.
Li, J., Wan, Y., Li, Y., Yao, G., Lai, B., 2019. Surface Fe(III)/Fe(II) cycle promoted the degradation of atrazine by peroxymonosulfate activation in the presence of hydroxylamine. Appl. Catal. B 256, 117782.
Li, T., Zhao, Z., Wang, Q., Xie, P., Ma, J., 2016. Strongly enhanced Fenton degradation of organic pollutants by cysteine: an aliphatic amino acid accelerator outweighs hydroquinone analogues. Water Res. 105, 479–486.
Lin, Z.-R., Zhao, L., Dong, Y.-H., 2017. Effects of low molecular weight organic acids and fulvic acid on 2,4,4′-trichlorobiphenyl degradation and hydroxyl radical formation in a goethite-catalyzed Fenton-like reaction. Chem. Eng. J. 326, 201–209.
Liu, X., Ji, H., Li, S., Liu, W., 2019. Graphene modified anatase/titanate nanosheets with enhanced photocatalytic activity for efficient degradation of sulfamethazine under simulated solar light. Chemosphere 233, 198–206.
Luo, L., Yao, Y., Gong, F., Huang, Z., Lu, W., Chen, W., Zhang, L., 2016a. Drastic enhancement on Fenton oxidation of organic contaminants by accelerating Fe(iii)/Fe(ii) cycle with l-cysteine. RSC Adv. 6, 47661–47668.
Luo, L., Yao, Y., Gong, F., Huang, Z., Lu, W., Chen, W., Zhang, L., 2016b. Drastic enhancement on Fenton oxidation of organic contaminants by accelerating Fe(iii)/Fe(ii) cycle with l-cysteine. RSC Adv. 6, 47661–47668.
Nie, C., Ao, Z., Duan, X., Wang, C., Wang, S., An, T., 2018. Degradation of aniline by electrochemical activation of peroxydisulfate at MWCNT cathode: the proofed concept of nonradical oxidation process. Chemosphere 206, 432–438.
Northup, A., Cassidy, D., 2008. Calcium peroxide (CaO2) for use in modified Fenton chemistry. J. Hazard. Mater. 152, 1164–1170.
Pan, Y., Su, H., Zhu, Y., Vafaei Molamahmood, H., Long, M., 2018. CaO_2 based Fenton-like reaction at neutral pH: accelerated reduction of ferric species and production of superoxide radicals. Water Res. 145, 731–740.
Peng, J., Wu, E., Wang, N., Quan, X., Sun, M., Hu, Q., 2019. Removal of sulfonamide antibiotics from water by adsorption and persulfate oxidation process. J. Mol. Liq. 274, 632–638.
Qin, W., Fang, G., Wang, Y., Zhou, D., 2018. Mechanistic understanding of polychlorinated biphenyls degradation by peroxymonosulfate activated with $CuFe_2O_4$ nanoparticles: key role of superoxide radicals. Chem. Eng. J. 348, 526–534.
Rahim Pouran, S., Abdul Raman, A.A., Wan Daud, W.M.A., 2014. Review on the application of modified iron oxides as heterogeneous catalysts in Fenton reactions. J. Clean. Prod. 64, 24–35.
Rivas-Ortiz, I.B., Cruz-González, G., Lastre-Acosta, A.M., Manduca-Artiles, M., Rapado-Paneque, M., Chávez-Ardanza, A., Teixeira, A.C.S.C., Jáuregui-Haza, U.J., 2017. Optimization of radiolytic degradation of sulfadiazine by combining Fenton and gamma irradiation processes. J. Radioanal. Nucl. 2597–2607 Ch. 314.
Rong, S.-P., Sun, Y.-B., Zhao, Z.-H., 2014. Degradation of sulfadiazine antibiotics by water falling film dielectric barrier discharge. Chin. Chem. Lett. 25, 187–192.
Subramanian, G., Madras, G., 2017. Remarkable enhancement of Fenton degradation at a wide pH range promoted by thioglycolic acid. Chem. Commun. (Camb.) 53, 1136–1139.
Sun, J., Wang, Q., Zhang, J., Wang, Z., Wu, Z., 2018. Degradation of sulfadiazine in drinking water by a cathodic electrochemical membrane filtration process. Electrochim. Acta 277, 77–87.
Wang, Y., Indrawirawan, S., Duan, X., Sun, H., Ang, H.M., Tadé, M.O., Wang, S., 2015. New insights into heterogeneous generation and evolution processes of sulfate radicals for phenol degradation over one-dimensional α-MnO_2 nanostructures. Chem. Eng. J. 266, 12–20.
Wang, Y., Feng, C., Li, Y., Gao, J., Yu, C.-P., 2017a. Enhancement of emerging contaminants removal using Fenton reaction driven by H_2O_2 -producing microbial fuel cells. Chem. Eng. J. 307, 679–686.
Wang, T., Zhou, Y., Cao, S., Lu, J., Zhou, Y., 2019a. Degradation of sulfanilamide by Fenton-like reaction and optimization using response surface methodology. Ecotoxicol. Environ. Saf. 172, 334–340.
Wang, H., Zhao, Y., Su, Y., Li, T., Yao, M., Qin, C., 2017b. Fenton-like degradation of 2,4-dichlorophenol using calcium peroxide particles: performance and mechanisms. RSC Adv. 7, 4563–4571.
Wang, D., Zhang, D., Xu, Q., Liu, Y., Wang, Q., Ni, B.-J., Yang, Q., Li, X., Yang, F., 2019b. Calcium peroxide promotes hydrogen production from dark fermentation of waste activated sludge. Chem. Eng. J. 355, 22–32.
Watts, R.J., Finn, D.D., Cutler, L.M., Schmidt, J.T., Teel, A.L., 2007. Enhanced stability of hydrogen peroxide in the presence of subsurface solids. J. Contam. Hydrol. 91, 312–326.
Wu, D., Bai, Y., Wang, W., Xia, H., Tan, F., Zhang, S., Su, B., Wang, X., Qiao, X., Wong, P.K., 2019. Highly pure MgO2 nanoparticles as robust solid oxidant for enhanced Fenton-like degradation of organic contaminants. J. Hazard. Mater. 374, 319–328.
Yan, J., Peng, J., Lai, L., Ji, F., Zhang, Y., Lai, B., Chen, Q., Yao, G., Chen, X., Song, L., 2018. Activation CuFe2O4 by hydroxylamine for oxidation of antibiotic sulfamethoxazole. Environ. Sci. Technol. 52, 14302–14310.
Yang, L., Shi, Y., Li, J., Fang, L., Luan, T., 2018a. Transformation of aqueous sulfonamides under horseradish peroxidase and characterization of sulfur dioxide extrusion products from sulfadiazine. Chemosphere 200, 164–172.
Yang, J.-F., He, M., Wu, T.-F., Hao, A.-P., Zhang, S.-B., Chen, Y.-D., Zhou, S.-B., Zhen, L.-Y., Wang, R., Yuan, Z.-L., Deng, L., 2018b. Sulfadiazine oxidation by permanganate: kinetics, mechanistic investigation and toxicity evaluation. Chem. Eng. J. 349, 56–65.
Yu, W., Yang, J., Shi, Y., Song, J., Shi, Y., Xiao, J., Li, C., Xu, X., He, S., Liang, S., Wu, X., Hu, J., 2016. Roles of iron species and pH optimization on sewage sludge conditioning with Fenton's reagent and lime. Water Res. 95, 124–133.
Zhang, Q.Q., Ying, G.G., Pan, C.G., Liu, Y.S., Zhao, J.L., 2015a. Comprehensive evaluation of antibiotics emission and fate in the river basins of China: source analysis, multimedia modeling, and linkage to bacterial resistance. Environ. Sci. Technol. 49, 6772–6782.
Zhang, C., Dong, Y., Li, B., Li, F., 2018a. Comparative study of three solid oxidants as substitutes of H_2O_2 used in Fe (III)-oxalate complex mediated Fenton system for photocatalytic elimination of reactive azo dye. J. Clean. Prod. 177, 245–253.
Zhang, Y., Klamerth, N., Gamal El-Din, M., 2016a. Degradation of a model naphthenic acid by nitrilotriacetic acid – modified Fenton process. Chem. Eng. J. 292, 340–347.
Zhang, X., Gu, X., Lu, S., Miao, Z., Xu, M., Fu, X., Qiu, Z., Sui, Q., 2015b. Degradation of trichloroethylene in aqueous solution by calcium peroxide activated with ferrous ion. J. Hazard. Mater. 284, 253–260.
Zhang, X., Gu, X., Lu, S., Miao, Z., Xu, M., Fu, X., Danish, M., Brusseau, M.L., Qiu, Z., Sui, Q., 2016b. Enhanced degradation of trichloroethene by calcium peroxide activated with Fe(III) in the presence of citric acid. Front. Environ. Sci. Eng. 10, 502–512.
Zhang, N., Wang, Q., Yuan, J., Cui, L., Wang, P., Yu, Y., Fan, X., 2018b. Highly efficient and eco-friendly wool degradation by L-cysteine-assisted esperase. J. Clean. Prod. 192, 433–442.
Zhou, Y., Zhang, R., Chen, K., Zhao, X., Gu, X., Lu, J., 2017a. Enhanced adsorption and photo-degradation of bisphenol A by β-cyclodextrin modified pine sawdust in an aquatic environment. J. Taiwan Inst. Chem. Eng. 78, 510–516.
Zhou, Y., Fang, X., Zhang, Zh., Hu, Y., Lu, J., 2017b. An oxygen slow-releasing material and its application in water remediation as oxygen supplier. Environ. Technol. 38 (22), 2793–2799.
Zhou, Y., Fang, X., Wang, T., Hu, Y., Lu, J., 2017c. Chelating agents enhanced CaO_2 oxidation of bisphenol A catalyzed by Fe^{3+} and reuse of ferric sludge as a source of catalyst. Chem. Eng. J. 313, 638–645.
Zou, X., Zhou, T., Mao, J., Wu, X., 2014. Synergistic degradation of antibiotic sulfadiazine in a heterogeneous ultrasound-enhanced Fe^0/persulfate Fenton-like system. Chem. Eng. J. 257, 36–44.